Hedgehog Spin-Vortex Crystal Antiferromagnetic Quantum Criticality in CaK(Fe$_{1-x}$Ni$_x$)$_4$As$_4$ Revealed by NMR

Q.-P. Ding,[1,2] W. R. Meier,[1,2] J. Cui,[1,3,*] M. Xu,[1,2] A. E. Böhmer,[1,2,†] S. L. Bud'ko,[1,2] P. C. Canfield,[1,2] and Y. Furukawa[1,2]

[1]*Ames Laboratory, U.S. DOE, Ames, Iowa 50011, USA*
[2]*Department of Physics and Astronomy, Iowa State University, Ames, Iowa 50011, USA*
[3]*Department of Chemistry, Iowa State University, Ames, Iowa 50011, USA*

Two ordering states, antiferromagnetism and nematicity, have been observed in most iron-based superconductors (SCs). In contrast to those SCs, the newly discovered SC CaK(Fe$_{1-x}$Ni$_x$)$_4$As$_4$ exhibits an antiferromagnetic (AFM) state, called hedgehog spin-vortex crystal (SVC) structure, without nematic order, providing the opportunity for the investigation into the relationship between spin fluctuations and SC without any effects of nematic fluctuations. Our ^{75}As nuclear magnetic resonance studies on CaK(Fe$_{1-x}$Ni$_x$)$_4$As$_4$ ($0 \leq x \leq 0.049$) revealed that CaKFe$_4$As$_4$ is located close to a hidden hedgehog SVC AFM quantum-critical point (QCP). The magnetic QCP without nematicity in CaK(Fe$_{1-x}$Ni$_x$)$_4$As$_4$ highlights the close connection of spin fluctuations and superconductivity in iron-based SCs. The advantage of stoichiometric composition also makes CaKFe$_4$As$_4$ an ideal platform for further detailed investigation of the relationship between magnetic QCP and superconductivity in iron-based SCs without disorder effects.

The relationship between antiferromagnetism (AFM), nematicity, and superconductivity in iron-based superconductors (SCs) has received wide interest [1–4]. The most controversial and important topic in iron-based SCs is the pairing mechanism, for which both spin and nematic fluctuations have been proposed, but no conclusion has been reached yet. SC in most iron pnictides appears in proximity to an AFM ordered state, which is closely accompanied by a nematic order. The SC critical temperature T_c shows a dome-shaped dependence on carrier doping or pressure application. Heavy fermions and high-T_c cuprates also exhibit similar phase diagrams [5,6]. In these compounds, normal-state properties often show a striking deviation from Landau's Fermi-liquid behavior near the optimal T_c composition [5–9]. The non-Fermi-liquid behavior, such as temperature- (T) linear resistivity has been discussed in terms of a quantum critical point (QCP) [7,10,11]. The existence of magnetic QCP has been reported in several iron-pnictide SCs, such as BaFe$_2$As$_2$-type (122) systems, for example, BaFe$_2$(As$_{1-x}$P$_x$)$_2$ [9,12], Ba(Fe$_{1-x}$M$_x$)$_2$As$_2$ (M = Co, Ni) [13–15]. However, recent NMR, μSR, and neutron scattering measurements indicate the presence of inhomogeneous AFM domains near optimal SC, suggesting an avoided QCP in electron-doped Ba(Fe$_{1-x}$M$_x$)$_2$As$_2$ [16–20]. The inhomogeneity presumably originates from the disorder due to Ni/Co substitutions. Even though substitutional disorder is not introduced on the Fe plane in BaFe$_2$(As$_{1-x}$P$_x$)$_2$, a recent study combined with NMR, x-ray, and neutron diffraction measurements also suggests an avoided QCP [21]. Thus, whether or not a

magnetic QCP exists in 122 compounds is still under debate. On the other hand, nematic fluctuations associated with nematic QCP have been increasingly suggested to enhance or even lead to SC in iron-based SCs, especially 122 systems [22–24].

Different from the 122 family, the newly discovered stoichiometric iron-based SC CaKFe$_4$As$_4$ with $T_c \sim 35$ K adopts a structure where the Fe-As layers are separated by alternate Ca and K planes [25,26]. The segregation of Ca and K is driven by their dissimilar sizes and reduces the space group from $I4/mmm$ in 122 compounds to $P4/mmm$ in CaKFe$_4$As$_4$. Consequently, as shown in the left-hand panel of Fig. 1, there are two inequivalent As sites: As1 and
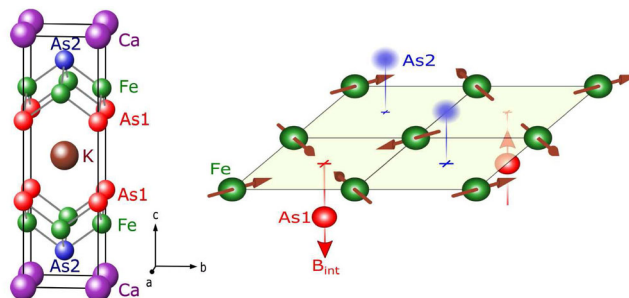

FIG. 1. The crystal structure of CaKFe$_4$As$_4$ (left) and the sketch of hedgehog SVC spin structure on an Fe-As layer (right). The wine-colored arrows represent the magnetic moments at the Fe sites and the red arrows represent the magnetic induction B_{int} at the As1 sites.

As2 sites close to the K and Ca layers, respectively. Other than SC, there is no indication of any other phase transition from 1.5 to 300 K [26,27]. The multiband nature of the compound and $s\pm$ nodeless two-gap SC state has been revealed by various techniques [28–32]. Quite recently, a new magnetic state called hedgehog spin-vortex crystal (SVC) with tetragonal symmetry, as shown in the right-hand panel of Fig. 1, has been discovered in the electron-doped SC $CaK(Fe_{1-x}M_x)_4As_4$ ($M = Co$ or Ni) [33]. The magnetic phase transition has been shown to be second order [33]. The subsequent NMR and neutron diffraction studies clearly evidenced the microscopic coexistence of the hedgehog SVC and SC [34,35]. As the phase diagram of $CaK(Fe_{1-x}M_x)_4As_4$ is revealed to be similar to that of doped 122 systems [33], it is interesting to search for a QCP in the new system.

In this Letter, we show the experimental evidence which suggests that a hidden AFM QCP exists around $x = 0$ from systematic ^{75}As NMR measurements on $CaK(Fe_{1-x}Ni_x)_4As_4$ single crystals. In particular, this is the first indication of a QCP with the newly discovered hedgehog SVC state. Nematic order and associated fluctuations, as well as the disorder caused by substitution, are absent in the stoichiometric SC $CaKFe_4As_4$ [36]. This makes $CaKFe_4As_4$ ideal for investigation into the potential link between spin fluctuations and superconductivity near the QCP without any effects from the nematic fluctuations and/or disorder [37]. The details of the NMR spectrum and nuclear spin-lattice relaxation rate $1/T_1$ data in the hedgehog SVC magnetic state for $x = 0.049$ and also in the SC state for $x = 0$ have been reported previously [28,34]. In this Letter, we mainly report the NMR data in the paramagnetic (PM) state and discuss the evolution of the hedgehog SVC spin correlations with Ni substitution.

Single crystals of $CaK(Fe_{1-x}Ni_x)_4As_4$ for the NMR measurements were grown out of a high-temperature solution rich in transition metals and arsenic [26,33,38]. Ni concentration was determined by wavelength-dispersive x-ray spectroscopy [33]. NMR measurements of ^{75}As ($I = \frac{3}{2}$, $\gamma_N/2\pi = 7.2919$ MHz/T, $Q = 0.29$ b) nuclei were conducted using a lab-built phase-coherent spin-echo pulse spectrometer on four different compounds, pure ($T_c = 35$ K), 1.7% substitution ($T_c = 31$ K), 3.3% substitution ($T_c = 23$ K, $T_N = 45$ K), and 4.9% substitution ($T_c = 10$ K, $T_N = 52$ K) [33]. The ^{75}As-NMR spectra were obtained by sweeping the magnetic field H at fixed frequencies. The ^{75}As $1/T_1$ was measured with a saturation recovery method [39].

Figures 2(a) and 2(b) show the typical field-swept ^{75}As-NMR spectra of $CaK(Fe_{1-x}Ni_x)_4As_4$ in the PM state for two magnetic field directions, $H\parallel c$ axis and $H\parallel ab$ plane, respectively. As reported in the previous papers [28,33,34], the two sets of $I = 3/2$ quadrupole split lines, corresponding to the two inequivalent As sites, are observed for the four compounds, as shown in Fig. 2.
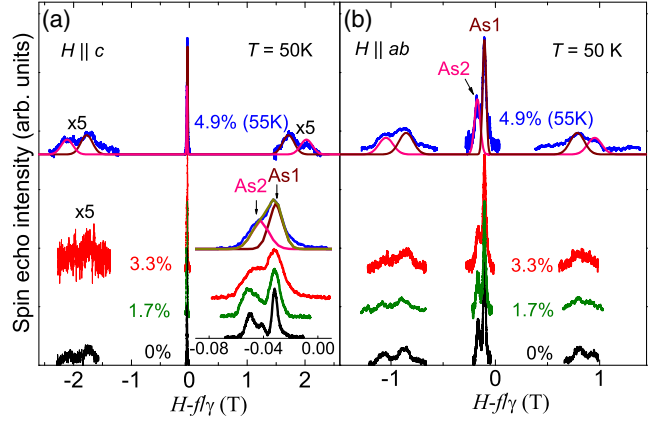

FIG. 2. Field-swept ^{75}As-NMR spectra of $CaK(Fe_{1-x}Ni_x)_4As_4$ at 50 K (55 K for 4.9% sample), for $H\parallel c$ axis (a) and $H\parallel ab$ plane (b). The inset in (a) enlarges the central transition. Pink and wine-colored curves represent simulated spectra for As1 and As2, respectively. The dark yellow in the inset of (a) represents the sum of the simulated spectra.

The lower field central peak with a greater Knight shift K (and also larger quadrupole frequency ν_Q) has been assigned to the As2 site close the Ca layers, and the higher field central peak with a smaller K (and also smaller ν_Q) has been attributed to the As1 site close to the K layers [28]. The clear separation of the two As NMR lines indicates that the well-ordered K and Ca layers are not disturbed by Ni substitution.

Figures 3(a) and 3(b) show the T dependence of K_{ab} ($H\parallel ab$ plane), K_c ($H\parallel c$ axis), and ν_Q for the two As sites. The As2 site K values are uniformly higher than the As1 site K values over the full temperature range. Because of the poor signal intensity at high T, ν_Q and K_{ab} can only be determined precisely up to 150–200 K. K_c, though, can be determined up to 300 K. For both the As sites, the K values are nearly independent of T, and also nearly independent
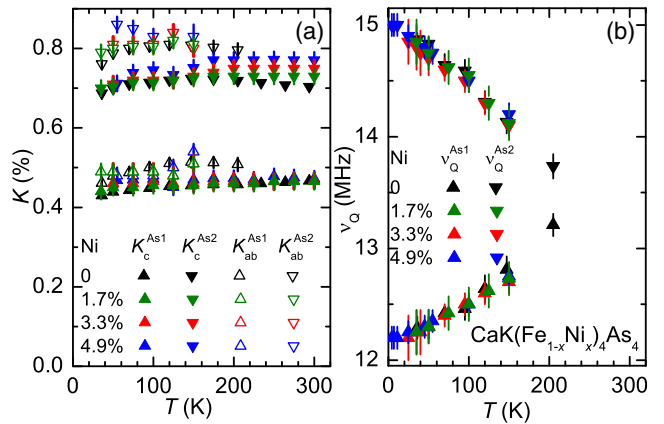

FIG. 3. (a) T dependences of the ^{75}As-NMR shifts K_c and K_{ab} for the As1 and As2 sites. (b) T dependences of quadrupole frequency ν_Q for the As1 and the As2 sites estimated from the NMR spectra.

of Ni substitution, indicating that static uniform magnetic susceptibility is nearly independent of both T and x, although the ground states vary from magnetic to non-magnetic. These data also suggest that Ni substitution up to 4.9% does not produce significant change in the density of states at the Fermi energy $N(E_F)$.

The T dependences of ν_Q of As1 and As2 in $CaK(Fe_{1-x}Ni_x)_4As_4$ are shown in Fig. 3(b). Similar to the K data, ν_Q is almost independent of Ni substitution. All the As2 ν_Q values are larger than the As1 ν_Q values. For all the samples, with increasing T, ν_Q of As1 increases, while ν_Q of As2 shows an opposite trend. The different T dependences of the values of ν_Q for the two As sites have been ascribed to hedgehog SVC magnetic fluctuations [28].

Figures 4(a)–4(d) show the T dependence of $1/T_1T$ for the two As sites under the different magnetic field directions. As can be seen, all $1/T_1T$ plots increase with decreasing T. $1/T_1T$ can be expressed in terms of the imaginary part of the dynamic susceptibility $\chi''(\vec{q}, \omega_0)$ at the Larmor frequency ω_0 per mole of electronic spins as [40] $1/T_1T = (2\gamma_N^2 k_B/N_A^2)\sum_{\vec{q}}|A(\vec{q})|^2[\chi''(\vec{q}, \omega_0)/\omega_0]$, where the sum is over the wave vectors $\vec{q}$ within the first Brillouin zone, $A(\vec{q})$ is the form factor of the hyperfine interactions. On the other hand, K reflects the $q = 0$ component of magnetic susceptibility $\chi'(\vec{q}, \omega_0)$. Therefore, the enhancement of $1/T_1T$ at low T where K is almost constant indicates a growth of AFM spin correlations with $q \neq 0$.

According to the previous analysis of $1/T_1T$ for $x = 0$ and 0.049 [28,34], the AFM spin correlations can be characterized to be hedgehog SVC correlations experimentally by the T dependence of the ratio of $1/T_1$ for As1 and $1/T_1$ for As2 [Figs. 4(e) and 4(f)]. In the hedgehog SVC ordered state, the internal magnetic induction B_{int} at As1 is finite along the c axis while the B_{int} at As2 is zero due to a cancellation originating from the characteristic spin structure [33,34]. Therefore, one expects that $1/T_1$ for As1 is enhanced compared to that of As2 if the AFM spin fluctuations originate from the hedgehog SVC-type spin correlations. For stripe-type AFM fluctuations, the T dependence of $1/T_1$ for As1 should scale to that of $1/T_1$ for As2 since there is no cancellation of the internal induction at either As site [33]. As can be seen in Figs. 4(e) and 4(f), the ratios of T_1^{As2}/T_1^{As1} show a nearly T-independent value of ~0.3–0.4 above 150 K, which could be determined by the different hyperfine coupling constants for the As1 and As2 sites. Below 150 K, clear enhancements of T_1^{As2}/T_1^{As1} are observed. These results indicate that the As1 sites experience stronger AFM spin fluctuations than the As2 sites, consistent with the growth of the hedgehog SVC spin fluctuations.

In order to get more insight into the hedgehog SVC spin fluctuations, we analyze the $1/T_1T$ data using a phenomenological model where $1/T_1T$ is decomposed into two components: $1/T_1T = (1/T_1T)_{AFM} + (1/T_1T)_0$ [12–15,41].
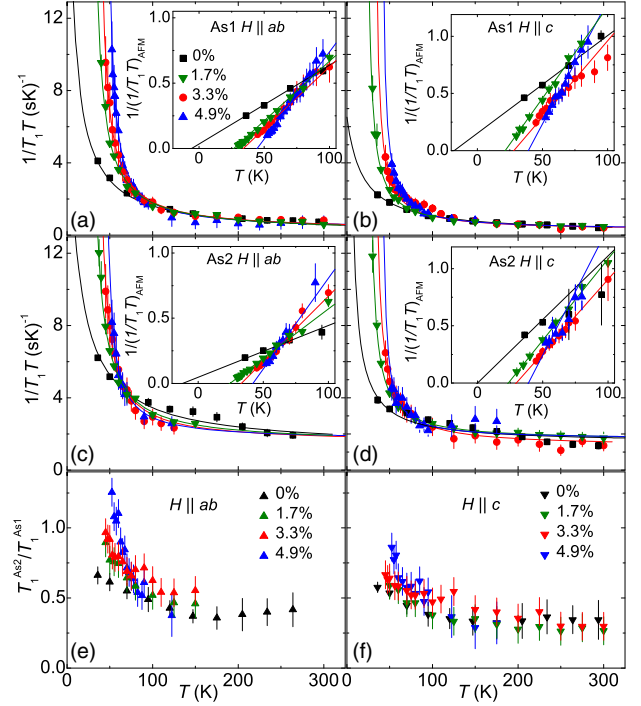

FIG. 4. T dependence of $1/T_1T$ of As1 site for $H\|ab$ plane (a) and $H\|c$ axis (b) and As2 site for $H\|ab$ plane (c) and $H\|c$ axis (d). The solid lines represent fits to $1/T_1T = C/(T + \theta) + const$ (see text). Insets: Inverse of the temperature-dependent component of $1/T_1T$. The intercepts of the linear fits with the x axis correspond to $-\theta$ (see text). T dependences of T_1^{As2}/T_1^{As1} for $H\|ab$ plane (e) and $H\|c$ axis (f).

Here, $(1/T_1T)_{AFM}$ is due to the AFM spin fluctuations which can be described by a Curie-Weiss formula $(1/T_1T)_{AFM} = C/(T + \theta)$ expected for an AFM spin fluctuation for a two-dimensional system from the self-consistent renormalization theory [40]. The Curie constant C measures the spectral weight of AFM fluctuations and the Weiss temperature θ corresponds to the distance from the AFM instability point. For the other term originating from a contribution other than the AFM correlations, we assumed $(1/T_1T)_0 = const$, which is expected for the Korringa relation of $T_1TK^2 = const$, since K is nearly constant. The solid lines in Figs. 4(a)–4(d) are fits for all $1/T_1T$ data. The Curie-Weiss behavior of $(1/T_1T)_{AFM}$ can also be seen clearly in the insets for each figure where the inverse of $(1/T_1T)_{AFM}$ follows T linear dependence.

Figure 5 shows the x dependence of θ and C estimated from the fits, together with the phase diagram of $CaK(Fe_{1-x}Ni_x)_4As_4$ [33]. As shown in the bottom panel, as x decreases, C increases and θ approaches zero. The increase of C suggests enhancement of the AFM fluctuations. A similar trend of T_c is observed, suggesting a correlation between C and T_c. On the other hand, as shown above, $N(E_F)$ in $CaK(Fe_{1-x}Ni_x)_4As_4$ changes little upon x, while T_c decreases as x increases. This is in contrast to the conventional BCS superconductors, in which $N(E_F)$

generally correlates with T_c. These results strongly, therefore, indicate that the hedgehog SVC spin fluctuations play an important role in the appearance of SC in CaKFe$_4$As$_4$. $\theta = 0$ K implies that the compound would show a hedgehog SVC magnetic order at 0 K if it remained in the normal state. This is an indication of an AFM QCP around $x = 0$ which is hidden or, as shown below, shifted by the appearance of SC below T_c.

In general, one expects that a magnetic QCP exists in proximity to an AFM phase boundary. For CaK(Fe$_{1-x}$Ni$_x$)$_4$As$_4$, therefore, an AFM state may be expected in the Ni-1.7% sample whose T_N is expected to be lower than T_c from a simple extrapolation of the values of T_N of the higher Ni concentration compounds. As shown in Figs. 3(a)–3(d), the strong divergent behavior in $1/T_1T$ with the negative θ value observed in the $T > T_c$ data for the Ni-1.7% sample is very similar to those observed at T_N for Ni-3.3% and Ni-4.9% samples, suggesting an AFM order in the Ni-1.7% doped sample. The determination of the ground state of the Ni-1.7% sample from the NMR spectrum measurements below T_c was difficult due to the poor NMR signal intensity originating from Meissner effect. However, as shown in the inset of the bottom panel of Fig. 5, specific-heat (C_p) measurements do not show any evidence of magnetic order below T_c in the Ni-1.7% doped sample where the clear jump in C_p at T_c can be detected [42]. These results indicate that no static magnetic order is established in the Ni-1.7% sample below T_c, and in a similar manner there is no magnetic order expected for $x \leq 0.017$. Similar sudden disappearance of the AFM state in the SC state has been observed in 122 families where the T_N line bent backwards into the AFM

region [2]. The absence of the magnetic order may originate from the strong competition with SC order in this region. The disappearance of magnetic order and/or the back-bending behavior of T_N have been discussed theoretically based on Ginzburg-Landau theory [43]. Although the actual AFM phase boundary in the SC state at low Ni-substitution levels does not change our conclusion of the hidden QCP around $x = 0$, which is revealed from the $1/T_1T$ data in the normal state, it is interesting and important to reveal the details of the phase diagram of CaK(Fe$_{1-x}$Ni$_x$)$_4$As$_4$. It would also be of great interest to investigate how the phase boundary changes if the SC is suppressed, for example, by strong magnetic field.

It is generally believed that, in proximity to an AFM QCP, the scattering process of quasiparticles is strongly affected by the quantum fluctuations, leading to non-Fermi-liquid behavior. As a result, electrical resistivity (ρ) increases linearly with temperature, which has been actually observed in high-T_c cuprates and some iron-based SCs around a QCP [7,9,11,12,15]. In the case of CaKFe$_4$As$_4$ [26], on the other hand, ρ is observed to be proportional to $T^{1.5}$, whose exponent is slightly higher than unity, but is clearly smaller than two which is expected for conventional Fermi liquid. Recently, the T-linear scattering rate of the coherent response [44] as a result of quantum fluctuations has been observed by an optical conductivity study of CaKFe$_4$As$_4$ [45], although the T-linear ρ is not observed. These results also support an existence of a magnetic QCP associated with the $T > T_c$ normal state, around CaKFe$_4$As$_4$.

The possibility of the avoided magnetic QCP in doped 122 compounds has been suggested by the observation of a distribution of T_1 and also of a secondary incommensurate magnetic phase near the optimal T_c [16–21]. In the case of CaKFe$_4$As$_4$, it is important to point out that we do not observe any distribution of T_1 in the normal state, indicative of no significant inhomogeneity. In addition, bulk measurements, μSR, and neutron scattering, as well as NMR, also rule out any magnetic phase in CaKFe$_4$As$_4$ [26–29]. Therefore, the stoichiometric CaKFe$_4$As$_4$ provides a unique opportunity to explore quantum criticality without the inherent substitutional disorder in analogous doped 122 systems. AFe$_2$As$_2$ (A = K, Rb, Cs) [46,47] and LiFeAs [48] are stoichiometric superconductors as well, and those systems are pointed out to be presumably located close to a magnetic instability. However, the maximum T_c in Ba$_{1-x}$K$_x$Fe$_2$As$_2$ appears at $x \sim 0.4$, not at the stoichiometric composition. LiFeAs shows a Fermi-liquid behavior, and no magnetic transitions has been detected in the temperature-doping (T-x) phase diagram of LiFe$_{1-x}$Co$_x$As [49]. These are quite different from CaK(Fe$_{1-x}$Ni$_x$)$_4$As$_4$.

In summary, our ^{75}As NMR measurements of CaK(Fe$_{1-x}$Ni$_x$)$_4$As$_4$ provide evidence for a QCP associated with hedgehog SVC fluctuations near $x = 0$. In contrast to other reported iron-based SCs with QCP, stoichiometric CaKFe$_4$As$_4$ is free of the substitutional disorder
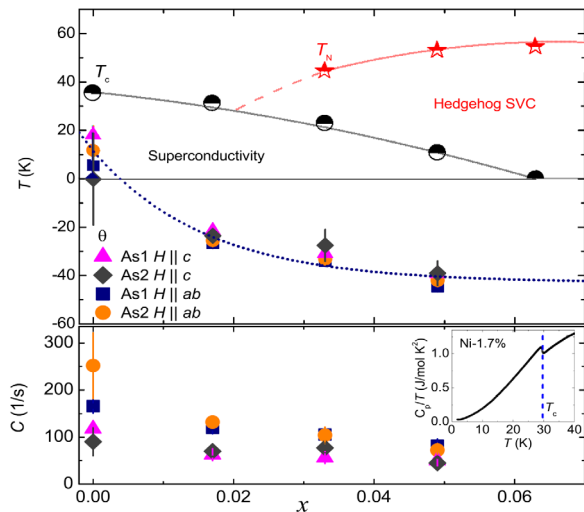

FIG. 5. Phase diagram of Ni-doped CaKFe$_4$As$_4$ (top). T_N and T_c are from Ref. [33]. Weiss temperature θ and Curie constant C (bottom) are obtained from the fits in Fig. 4. The lines are guides to the eye. The inset of the bottom panel shows the specific heat C_p/T of Ni-1.7% sample.

from chemical doping and also nematic transition. The magnetic QCP without accompanying nematicity in $CaK(Fe_{1-x}Ni_x)_4As_4$ highlights the close connection of spin fluctuations and SC in iron-based SCs. These advantages make $CaKFe_4As_4$ an ideal platform to investigate the relationship between magnetic QCP and SC in iron-based SCs.

---

[*]Present address: Department of Chemistry, University of Delaware, Newark, Delaware 9716, USA.

[†]Present address: Karlsruhe Institute of Technology, Institut für Festkörperphysik, 76021 Karlsruhe, Germany.

[1] P. C. Canfield and S. L. Bud'ko, Annu. Rev. Condens. Matter Phys. **1**, 27 (2010).

[2] D. C. Johnston, Adv. Phys. **59**, 803 (2010).

[3] P. J. Hirschfeld, M. M. Korshunov, and I. I. Mazin, Rep. Prog. Phys. **74**, 124508 (2011).

[4] G. R. Stewart, Rev. Mod. Phys. **83**, 1589 (2011).

[5] M. R. Norman, D. Pines, and C. Kallin, Adv. Phys. **54**, 715 (2005).

[6] C. Pfleiderer, Rev. Mod. Phys. **81**, 1551 (2009).

[7] D. M. Broun, Nat. Phys. **4**, 170 (2008).

[8] J. Dai, Q. Si, J.-X. Zhu, and E. Abrahams, Proc. Natl. Acad. Sci. U.S.A. **106**, 4118 (2009).

[9] T. Shibauchi, A. Carrington, and Y. Matsuda, Annu. Rev. Condens. Matter Phys. **5**, 113 (2014).

[10] S. Sachdev, *Quantum Phase Transitions* (Cambridge University Press, Cambridge, England, 1999).

[11] S. Sachdev and B. Keimer, Phys. Today **64**, No. 2, 29 (2011).

[12] Y. Nakai, T. Iye, S. Kitagawa, K. Ishida, H. Ikeda, S. Kasahara, H. Shishido, T. Shibauchi, Y. Matsuda, and T. Terashima, Phys. Rev. Lett. **105**, 107003 (2010).

[13] F. L. Ning, K. Ahilan, T. Imai, A. S. Sefat, R. Jin, M. A. Mcquire, B. C. Sales, and D. Mandrus, J. Phys. Soc. Jpn. **78**, 013711 (2009).

[14] F. L. Ning, K. Ahilan, T. Imai, A. S. Sefat, M. A. McGuire, B. C. Sales, D. Mandrus, P. Cheng, B. Shen, and H.-H Wen, Phys. Rev. Lett. **104**, 037001 (2010).

[15] R. Zhou, Z. Li, J. Yang, D. L. Sun, C. T. Lin, and G.-q. Zheng, Nat. Commun. **4**, 2265 (2013).

[16] A. P. Dioguardi, J. Crocker, A. C. Shockley, C. H. Lin, K. R. Shirer, D. M. Nisson, M. M. Lawson, N. apRoberts-Warren, P. C. Canfield, S. L. Bud'ko, S. Ran, and N. J. Curro, Phys. Rev. Lett. **111**, 207201 (2013).

[17] X. Lu, D. W. Tam, C. Zhang, H. Luo, M. Wang, R. Zhang, L. W. Harriger, T. Keller, B. Keimer, L.-P. Regnault, T. A. Maier, and P. Dai, Phys. Rev. B **90**, 024509 (2014).

[18] C. Bernhard, C. N. Wang, L. Nuccio, L. Schulz, O. Zaharko, J. Larsen, C. Aristizabal, M. Willis, A. J. Drew, G. D. Varma, T. Wolf, and Ch. Niedermayer, Phys. Rev. B **86**, 184509 (2012).

[19] H. Luo, R. Zhang, M. Laver, Z. Yamani, M. Wang, X. Lu, M. Wang, Y. Chen, S. Li, S. Chang, J. W. Lynn, and P. Dai, Phys. Rev. Lett. **108**, 247002 (2012).

[20] X. Lu, H. Gretarsson, R. Zhang, X. Liu, H. Luo, W. Tian, M. Laver, Z. Yamani, Y.-J. Kim, A. H. Nevidomskyy, Q. Si, and P. Dai, Phys. Rev. Lett. **110**, 257001 (2013).

[21] D. Hu, X. Lu, W. Zhang, H. Luo, S. Li, P. Wang, G. Chen, F. Han, S. R. Banjara, A. Sapkota, A. Kreyssig, A. I. Goldman, Z. Yamani, C. Niedermayer, M. Skoulatos, R. Georgii, T. Keller, P. Wang, W. Yu, and P. Dai, Phys. Rev. Lett. **114**, 157002 (2015).

[22] S. Lederer, Y. Schattner, E. Berg, and S. A. Kivelson, Phys. Rev. Lett. **114**, 097001 (2015).

[23] Y. Schattner, S. Lederer, S. A. Kivelson, and E. Berg, Phys. Rev. X **6**, 031028 (2016).

[24] Z. Liu, Y. Gu, W. Zhang, D. Gong, W. Zhang, T. Xie, X. Lu, X. Ma, X. Zhang, R. Zhang, J. Zhu, C. Ren, L. Shan, X. Qiu, P. Dai, Y.-F. Yang, H. Luo, and S. Li, Phys. Rev. Lett. **117**, 157002 (2016).

[25] A. Iyo, K. Kawashima, T. Kinjo, T. Nishio, S. Ishida, H. Fujihisa, Y. Gotoh, K. Kihou, H. Eisaki, and Y. Yoshida, J. Am. Chem. Soc. **138**, 3410 (2016).

[26] W. R. Meier, T. Kong, U. S. Kaluarachchi, V. Taufour, N. H. Jo, G. Drachuck, A. E. Böhmer, S. M. Saunders, A. Sapkota, A. Kreyssig, M. A. Tanatar, R. Prozorov, A. I. Goldman, F. F. Balakirev, A. Gurevich, S. L. Bud'ko, and P. C. Canfield, Phys. Rev. B **94**, 064501 (2016).

[27] T. Xie, Y. Wei, D. Gong, T. Fennell, U. Stuhr, R. Kajimoto, K. Ikeuchi, S. Li, J. Hu, and H. Luo, Phys. Rev. Lett. **120**, 267003 (2018).

[28] J. Cui, Q.-P. Ding, W. R. Meier, A. E. Böhmer, T. Kong, V. Borisov, Y. Lee, S. L. Bud'ko, R. Valentí, P. C. Canfield, and Y. Furukawa, Phys. Rev. B **96**, 104512 (2017).

[29] P. K. Biswas, A. Iyo, Y. Yoshida, H. Eisaki, K. Kawashima, and A. D. Hillier, Phys. Rev. B **95**, 140505 (2017).

[30] K. Cho, A. Fente, S. Teknowijoyo, M. A. Tanatar, K. R. Joshi, N. M. Nusran, T. Kong, W. R. Meier, U. Kaluarachchi, I. Guillamón, H. Suderow, S. L. Bud'ko, P. C. Canfield, and R. Prozorov, Phys. Rev. B **95**, 100502 (2017).

[31] D. Mou, T. Kong, W. R. Meier, F. Lochner, L.-L. Wang, Q. Lin, Y. Wu, S. L. Bud'ko, I. Eremin, D. D. Johnson, P. C. Canfield, and A. Kaminski, Phys. Rev. Lett. **117**, 277001 (2016).

[32] K. Iida, M. Ishikado, Y. Nagai, H. Yoshida, A. D. Christianson, N. Murai, K. Kawashima, Y. Yoshida, H. Eisaki, and A. Iyo, J. Phys. Soc. Jpn. **86**, 093703 (2017).

[33] W. R. Meier, Q.-P. Ding, A. Kreyssig, S. L. Bud'ko, A. Sapkota, K. Kothapalli, V. Borisov, R. Valentí, C. D. Batista, P. P. Orth, R. M. Fernandes, A. I. Goldman, Y. Furukawa, A. E. Böhmer, and P. C. Canfield, npj Quantum Mater. **3**, 5 (2018).

[34] Q.-P. Ding, W. R. Meier, A. E. Böhmer, S. L. Bud'ko, P. C. Canfield, and Y. Furukawa, Phys. Rev. B **96**, 220510(R) (2017).

[35] A. Kreyssig, J. M. Wilde, A. E. Böhmer, W. Tian, W. R. Meier, B. Li, B. G. Ueland, M. Xu, S. L. Bud'ko, P. C. Canfield, R. J. McQueeney, and A. I. Goldman, Phys. Rev. B **97**, 224521 (2018).

[36] W.-L. Zhang, W. R. Meier, T. Kong, P. C. Canfield, and G. Blumberg, arXiv:1804.06963.

[37] Y. Gu, Z. Liu, T. Xie, W. Zhang, D. Gong, D. Hu, X. Ma, C. Li, L. Zhao, L. Lin, Z. Xu, G. Tan, G. Chen, Z. Y. Meng, Y.-F. Yang, H. Luo, and S. Li, Phys. Rev. Lett. **119,** 157001 (2017).

[38] W. R. Meier, T. Kong, S. L. Bud'ko, and P. C. Canfield, Phys. Rev. Mater. **1,** 013401 (2017).

[39] See Supplemental Material at http://link.aps.org/supplemental/10.1103/PhysRevLett.121.137204 for details for the determination of T_1 and the position dependence of T_1.

[40] T. Moriya, J. Phys. Soc. Jpn. **18,** 516 (1963).

[41] J. Cui, B. Roy, M. A. Tanatar, S. Ran, S. L. Bud'ko, R. Prozorov, P. C. Canfield, and Y. Furukawa, Phys. Rev. B **92,** 184504 (2015).

[42] The heat capacity data of the Ni-1.7% sample was measured using a hybrid adiabatic relaxation technique of the heat capacity option in a Quantum Design, Physical Properties Measurement System.

[43] R. M. Fernandes and J. Schmalian, Phys. Rev. B **82,** 014521 (2010).

[44] Y. M. Dai, B. Xu, B. Shen, H. Xiao, H. H. Wen, X. G. Qiu, C. C. Homes, and R. P. S. M. Lobo, Phys. Rev. Lett. **111,** 117001 (2013).

[45] R. Yang, Y. Dai, B. Xu, W. Zhang, Z. Qiu, Q. Sui, C. C. Homes, and X. Qiu, Phys. Rev. B **95,** 064506 (2017).

[46] Z. T. Zhang, D. Dmytriieva, S. Molatta, J. Wosnitza, S. Khim, S. Gass, A. U. B. Wolter, S. Wurmehl, H.-J. Grafe, and H. Kühne, Phys. Rev. B **97,** 115110 (2018).

[47] Y. P. Wu, D. Zhao, A. F. Wang, N. Z. Wang, Z. J. Xiang, X. G. Luo, T. Wu, and X. H. Chen, Phys. Rev. Lett. **116,** 147001 (2016).

[48] S.-H. Baek, L. Harnagea, S. Wurmehl, B. Büchner, and H.-J. Grafe, J. Phys. Condens. Matter **25,** 162204 (2013).

[49] Y. M. Dai, H. Miao, L. Y. Xing, X. C. Wang, P. S. Wang, H. Xiao, T. Qian, P. Richard, X. G. Qiu, W. Yu, C. Q. Jin, Z. Wang, P. D. Johnson, C. C. Homes, and H. Ding, Phys. Rev. X **5,** 031035 (2015).